LIMNOLOGY and OCEANOGRAPHY

Limnol. Oceanogr. 9999, 2020, 1–11

doi: 10.1002/lno.11565

Physiological and molecular responses to ocean acidification among strains of a model diatom

Ruiping Huang,[1] Jiancheng Ding,[2] Jiazhen Sun,[1] Yang Tian,[1] Chris Bowler,[3] Xin Lin,[1,4*] Kunshan Gao [1]

[1]State Key Laboratory of Marine Environmental Science and College of Ocean and Earth Sciences, Xiamen University, Xiamen, China

[2]School of Pharmaceutical Sciences, Xiamen University, Xiamen, China

[3]Institut de Biologie de l'ENS (IBENS), Département de Biologie, École Normale Supérieure, CNRS, INSERM, Université PSL, Paris, France

[4]Xiamen City Key Laboratory of Urban Sea Ecological Conservation and Restoration (USER), Xiamen, China

Abstract

Differential responses of diatoms, an important group of marine primary producers to ocean acidification, have been well documented. However, studies so far are based on limited representative strains from key species. Investigation of strain level responses will help us better understand the contrasting discrepancy in diatom responses to ocean acidification. Here, we selected four strains of the model diatom *Phaeodactylum tricornutum* isolated from different regions of the global ocean, representing all genotypes based on internal transcribed spacer 2 sequences, and investigated strain-specific responses to ocean acidification. In response to ocean acidification, changes in carbon metabolism varied among strains, although no significant effects of ocean acidification on growth rates or pigments were observed in any strains. The expression of genes encoding plasma membrane bicarbonate transporters was downregulated in strain Pt4, reflecting a potential decrease in active HCO_3^- uptake, which was not observed in the other strains. Reduction of CO_2 concentrating mechanism efficiency was also indicated by the regulated expression of genes encoding carbonic anhydrases that catalyze the interconversion of HCO_3^- and CO_2 in the pyrenoids and pyrenoid-penetrating thylakoid, which exhibited different patterns among the strains. Under ocean acidification conditions, C4-like metabolism appeared to redistribute carbon flux to gluconeogenesis in strain Pt1, and lipid synthesis in strains Pt8 and Pt11, rather than participating in net photosynthetic carbon fixation. These variations were incompletely correlated with phylogenetic relationship in different strains, implying that the habitat-adapted imprints of the different strains could also be responsible for their differential responses to ocean acidification.

Diatoms are responsible for about 40% of ocean primary production and play crucial roles in the biogeochemical cycles of carbon and silicon (Kiene 2008). However, the concentrations of CO_2 in contemporary surface oceans ($\sim$ 10–25 μmol L^{-1}) are much lower than the Michaelis-Menten half saturation constant for CO_2 (23–68 μmol L^{-1}) of diatom ribulose-1,5-biphosphate carboxylase/oxygenase (Rubisco) (Young et al. 2016). Diatoms have therefore evolved CO_2 concentrating mechanisms (CCMs) that overcome CO_2 limitation (Badger et al. 1998), which include passive CO_2 influx and active HCO_3^- influx at the plasma membrane, and then transport of HCO_3^- from the cytoplasm into the chloroplasts. Carbonic anhydrases (CAs), catalyzing the interconversion of CO_2 and HCO_3^-, play vital roles in the process of dissolved inorganic carbon (DIC) uptake from the environment to the chloroplasts (Hopkinson et al. 2016; Raven and Beardall 2016). It has been shown that ongoing increases in seawater CO_2 and HCO_3^-, as a consequence of ocean acidification (Gattuso et al. 2015), influence many marine organisms (Kroeker et al. 2013), phytoplankton community structure (Gao et al. 2012) and biogeochemical cycles (Gehlen et al. 2011). Contrasting findings have shown that ocean acidification may stimulate, inhibit, or have no influence on growth rates of diatoms (*see* Gao and Campbell 2014, and references therein).

Responses of diatoms to ocean acidification are usually modulated by other environmental drivers, such as light fluctuation (Hoppe et al. 2015), carbonate chemistry fluctuation (Li et al. 2016), nutrient limitation (Li et al. 2018), and

*Correspondence: xinlinulm@xmu.edu.cn

Additional Supporting Information may be found in the online version of this article.

Author Contribution Statement: X.L., R. H., and K.G. planned and designed the research. R.H., J.S., and Y.T. performed experiments. R.H. and J.D. analyzed data. R.H. wrote manuscript. X.L., C.B., and K.G. revised manuscript.

temperature (Torstensson et al. 2013). In the model diatom *Phaeodactylum tricornutum*, constant white fluorescence light with intensity of 200–460 μmol photons m^{-2} s^{-1} resulted in higher extents of growth enhancement by high CO_2 (1000 μatm) (Li et al. 2014; Liu et al. 2017). However, the enhancement of growth rates in this diatom by high CO_2 was offset or even reversed when the cells were grown under conditions of natural fluctuated sunlight with 200–450 μmol photons m^{-2} s^{-1} daytime mean photosynthetic active radiation (Gao et al. 2012). Previous results also have shown that ocean acidification interacts antagonistically with nitrate limitation and UV radiation to reduce photosynthetic performance of *P. tricornutum* (Li et al. 2015), but when combined with warming it synergistically increased physiological performance (Li et al. 2012).

Diatoms are known to exhibit diversified mechanisms for acquisition of inorganic carbon. In the Antarctic diatoms *Chaetoceros debilis*, *Pseudo-nitzschia subcurvata*, and *Fragilariopsis kerguelensis*, predominant HCO_3^- uptake has shown to positively correlate with extracellular CAs activity in response to high CO_2, supporting the hypothesis that extracellular CAs convert CO_2 leaking out of the cell to HCO_3^- that is subsequently taken up by HCO_3^- transporters (Trimborn et al. 2013). In addition, Tsuji et al. 2017 indicated the occurrence of two distinct strategies for DIC uptake in diatoms: one primary facilitated by HCO_3^- transporter and the other being passive CO_2 entry facilitated by external CA. These two distinct strategies have shown to be phylogenetically independent, implying that the evolution of distinct carbon acquisition mechanisms in different diatom species may be driven by environment rather than species phylogeny (Tsuji et al. 2017).

The DIC transport and interconversion of HCO_3^- and CO_2 constitute biophysical CCMs. Biochemical CCMs are characterized by the carboxylation of C3 compounds to form C4 compounds and providing CO_2 via decarboxylating C4 compounds in close proximity to Rubisco. It is generally considered that C4-like metabolism can function as biochemical CCMs in the marine centric diatom *Thalassiosira weissflogii* (Reinfelder et al. 2000; Roberts et al. 2007). However, the existence of biochemical CCMs in another marine centric diatom *Thalassiosira pseudonana* is still controversial. The tracer experiment has indicated that *T. pseudonana* may not possess biochemical CCMs, since no C4 compounds, produced by carboxylating C3 compounds, were detected in the major initial photosynthetic products (Roberts et al. 2007). However, low CO_2 (7.1 μmol L^{-1}) has shown to rearrange the transcriptional pattern of the genes encoding proteins involving C4-like metabolism, which may result in increasing CO_2 supply for carbon fixation, indicating the existence of biochemical CCMs in *T. pseudonana* (Kustka et al. 2014). It is considered that *P. tricornutum* may not possess functional biochemical CCMs. Previous studies have shown that no decarboxylases localized in the chloroplast are detected, although *P. tricornutum* encodes enzymes involved in carboxylation and decarboxylation in C4-like metabolism (Kroth et al. 2008; Ewe et al. 2018). Haimovich-Dayan et al. 2013 also showed that C4-like metabolism may not serve for raising CO_2 concentration in close proximity of Rubisco in *P. tricornutum*, because the photosynthetic half saturation constant for CO_2 was hardly affected in pyruvate-orthophosphate dikinase (PPDK) silenced cells.

Furthermore, the environments that are inhabited by different strains of the same diatom species are extremely variable. One example of a fluctuating parameter is light conditions in different isolated locations, which may contribute to different response strategies to light among strains of *P. tricornutum* (Bailleul et al. 2010). On the other hand, variation in responses to high CO_2 among strains of the same diatom species has rarely been documented (McCarthy et al. 2012). Previous studies have shown that the magnitudes of these responses varied among strains of the coccolithophore *Emiliania huxleyi* (Langer et al. 2009; Müller et al. 2015), the prasinophyte *Ostreococcus tauri* (Schaum et al. 2012), and the cyanobacterium *Crocosphaera watsonii* (Hutchins et al. 2013). The variation in responses to climate change-related parameters among strains could be attributed to the environmental conditions where the phytoplankton species were isolated (Schaum et al. 2012). On the other hand, it was thought that such variations could have a genetic basis (Langer et al. 2009; Zhang et al. 2014), although the underlying molecular mechanisms are still unknown. Therefore, the variation among strains of diatoms in response to rising CO_2 and the underlying mechanisms are worth to be explored.

Phaeodactylum tricornutum is a well-studied model diatom species with 11 strains isolated worldwide (De Martino et al. 2007; Wu et al. 2010). The morphological characteristics, genetic polymorphism, structure and functional diversity, variations in response to salinity, nutrients and temperatures have been examined for each strain (De Martino et al. 2007, 2011; Abida et al. 2015; Rastogi et al. 2019), except for one strain isolated more recently from the South China Sea. In this study, we grew four *P. tricornutum* strains at ambient and high pCO_2 levels to investigate their physiological and molecular responses to ocean acidification. Our results show that the strain-specific responses among four *P. tricornutum* strains in respect of carbon metabolism both at physiological and molecular levels are probably correlated with habitat-adapted imprints. This study provides a better understanding of variation in responses to high CO_2 among strains of the same diatom species and their underlying molecular mechanisms.

Materials and methods

Strain selection and growth conditions

The four *P. tricornutum* strains used in this study were Pt1 (isolated from the Irish Sea, UK in 1956), Pt4 (isolated from the Baltic Sea, Finland in 1951), Pt8 (isolated from the Salish

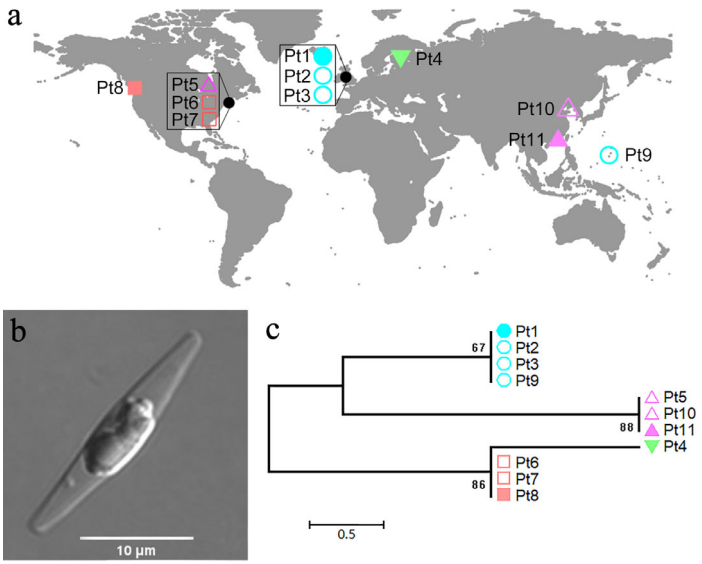

Fig. 1. Ecological distribution, morphological characteristics and phylogenetic analysis of the *P. tricornutum* strain Pt11. (**a**) Analysis of *P. tricornutum* strains isolated from different locations; (**b**) The morphological characteristics of Pt11, photographs were taken by confocal microscope; (**c**) Phylogenetic tree of *P. tricornutum* by the neighbor-joining method with 1000 bootstrap replicates based on analysis of the ITS2 sequences. Different colors represent different genotypes, and strains with solid circles were selected for the current study.

Sea, Canada in 1987), and Pt11 (isolated from the South China Sea, China in 2004) (Fig. 1a). These axenic strains were cultured in glass flasks containing 350 mL artificial seawater enriched with Aquil medium, which included 100 μmol L^{-1} nitrate and 10 μmol L^{-1} phosphate, at 20°C and 120 μmol photons m^{-2} s^{-1} with a 12 h light : 12 h dark photoperiod. The seawater was aerated using ambient air (410 ppmv; denoted AC) or premixed air containing higher levels of CO_2 (1000 ppmv; denoted HC), and pCO_2 was monitored using a CO_2 meter (GM70, Vaisala, Finland). The diatoms were semi-continuously cultured within a range of 1×10^4 to approximately 3×10^5 cells mL^{-1} by aerating AC and HC gas at a flow rate of 0.3 L min^{-1}, to maintain the stable carbonate system. Each treatment was performed in triplicate for each strain. Changes in seawater pH were measured before and after dilution using a pH meter (Orion 2, Thermo, U.S.A.). Physiological and molecular experiments were performed until strains were acclimated to AC and HC conditions for more than 15 generations.

Morphology, growth rate, and pigment content

The length and width of 20 live cells from each sample were measured using a confocal microscope (A1R HD25, Nikon, Japan), and the mean cell volumes were calculated assuming a prism on an elliptic base (Hillebrand et al. 1999). Cell concentrations were measured using a particle count and size analyzer (Z2 Coulter, Beckman, U.S.A.). The specific growth rate (μ, d^{-1}) was calculated according to the equation: $\mu = (\ln C_1 - \ln C_0)/(t_1 - t_0)$, in which C_0 and C_1 represent the cell concentrations at Day t_0 and Day t_1, respectively. Pigment contents were determined spectrophotometrically. Cells were filtered onto GF/F membranes (Whatman, UK) with low vacuum pressure (less than 0.01 MPa) and immersed in pure methanol overnight at 4°C in darkness. Extracts were centrifuged at $5000 \times g$ for 10 min, and the absorption spectra of the supernatants were measured using a UV-VIS Spectrophotometer (DU800, Beckman, U.S.A.). The concentrations of chlorophyll *a* (Chl *a*) and carotenoids were calculated according to the equations from Ritchie (2006) and Strickland and Parsons (1972).

DIC affinity

The photosynthesis vs. DIC curves (P-C curves) were determined by measuring photosynthetic O_2 evolution rate using a Clark-type oxygen electrode (Hansatech, UK) at 20°C. Cultured cells were filtered onto 2 μm polycarbonate membranes (Millipore, U.S.A.) by vacuum filtration with a pressure of less than 0.01 MPa. The collected cells were washed and resuspended in DIC-free artificial seawater buffered with 20 mmol L^{-1} Tris-HCl (pH = 8.15) at a cell concentration of approximately 2×10^6 cells mL^{-1}. 1.5 mL of cell suspension were placed into the chamber and illuminated with a white fluorescence light of 400 μmol photons m^{-2} s^{-1} to exhaust the possible intracellular inorganic carbon pool until net oxygen evolution rate reached near-zero. Subsequently, as $NaHCO_3$ was added progressively into the chamber at a final concentration of DIC within a range of 0–8 mmol L^{-1}, oxygen evolution rates were measured. The half saturation constants ($K_{1/2}$, μmol L^{-1}) and the maximum photosynthetic oxygen evolution rates (V_{max}, fmol O_2 $cell^{-1}$ h^{-1}) were calculated by fitting P-C curves with the Michaelis-Menten equation.

DNA extraction and internal transcribed spacer 2 sequencing

Cells of each strain were harvested by centrifugation for 10 min at $4000 \times g$ and 4°C, washed with 2 mL of phosphate-buffered saline buffer (0.01 mol L^{-1}, pH = 7.4) into 2 mL Eppendorf tubes, and then pelleted for 10 min at $4000 \times g$. Subsequently, 900 μL of lysis buffer, containing 10 μg mL^{-1} proteinase K, was added to the cell pellets. The extracts were incubated for 30 min at 37°C followed by centrifuged for 10 min at $4000 \times g$, and the supernatant was transferred into new 2 mL Eppendorf tube. Then DNA was extracted by phenol-chloroform extraction method, and purified with genomic DNA clean & concentrator™-10 (Zymo, U.S.A.) according to manufacturer protocol.

The partial rDNA region of Pt11, containing partial 3′ end of 5.8S, completed internal transcribed spacer 2 (ITS2), and partial 5′ end of 28S rDNA, was amplified by high-fidelity polymerase chain reaction (PCR) with forward primer ITS3

(5′-gcatcgatgaagaacgcagc-3′), reverse primer TW13 (5′-ggtccgtgtttcaagacg-3′) and PrimeSTAR Max DNA polymerase (Takara, China) (De Martino et al. 2007). Subsequently, the purified PCR fragment was sequenced. The hypervariable ITS2 sequences of Pt11 and other 10 *P. tricornutum* strains previously published in De Martino et al. 2007 were used to construct a phylogenetic tree by the neighbor-joining method with 1000 bootstrap replicates.

RNA extraction and quantitative reverse transcription PCR

Cells cultured under the AC or HC conditions were collected onto 2 μm polycarbonate membranes (Millipore) by vacuum filtration with a pressure of less than 0.01 MPa, resuspended into 1.5 mL of culture solution, and centrifuged for 10 min at $4000 \times g$ and 4°C. The cell pellets were frozen quickly with liquid nitrogen and stored at −80°C. Total RNA of frozen cells was extracted with TRIzol reagent (MRC, U.S.A.) and purified with RNA clean & concentrator™-5 (Zymo, U.S.A.). For the single strand cDNA synthesis, total RNA was reverse transcribed using PrimerScript™ RT reagent Kit with gDNA Eraser (Perfect Real Time, Takara, China) following manufacturer's protocol. The amplification specification and efficiency of primers, as well as the expression levels of the genes involved in biophysical CCMs and C4-like metabolism, were detected by CFX96™ Real-Time System (Bio-Rad, U.S.A.) using SYBR® Premix Ex Taq™ II (Tli RNaseH Plus, Takara, China) with primer concentration of 0.4 μmol L^{-1} each according to manufacturer's protocol. Primers used for qRT-PCR were designed according to genomic resequencing data with Beacon Designer 7, and listed in Supporting Information Table S1. Each qRT-PCR was conducted in triplicate as follows: 95°C for 60 s, followed by 40 cycles of 95°C for 10 s and 60°C for 30 s. Dissociation curves, which detect primer amplification specification, were generated by heating samples from 60°C to 95°C with an increment of 0.5°C every 5 s. Primer amplification efficiency was calculated by linear fitting standard curves of C_T and $\log_{(\text{starting quantity})}$, and listed in Supporting Information Table S1. The relative transcriptional level of target genes was normalized to reference gene ribosomal protein small subunit 30S (Siaut et al. 2007), according to the equation: $\text{Ratio}_{(\text{Target/Reference})} = 2^{(C_T(\text{Reference}) - C_T(\text{Target}))}$.

Statistics

Statistical analyses were performed using SPSS 19.0 (SPSS, Chicago, Illinois, U.S.A.). Prior to all statistical analyses, the homogeneity of variance was examined using Levene's test. One-way analysis of variance (ANOVA) was employed to check the effects of individual factors pCO_2 and strains, and then Fisher's least significant difference was used to determine variations in these four strains. Statistical significance was determined at the level of p value less than 0.05.

Results

Basic characteristics of Pt11

Except for Pt11, the morphological, geographical, and genomic information of Pt1, Pt4, and Pt8 have been well documented in De Martino et al. (2007) and Rastogi et al. (2019). Pt11 was isolated from South China Sea in 2004, and deposited at the Center for Collections of Marine Bacteria and Phytoplankton (CCMA106, Xiamen University, China). Pt11 is fusiform, with 22.9 ± 0.9 μm in length and 3.5 ± 0.2 μm in width (Fig. 1b). The sequence containing partial 3′ end of 5.8S, completed ITS2, and partial 5′ end of 28S rDNA of Pt11 has been deposited in GenBank (MK585217). The ITS2 sequence of Pt11 showed 98–100% similarity with the other 10 *P. tricornutum* strains. The nucleotides at +195, +327, +431, +444, +476, and +488 site of Pt11 partial rDNA regions submitted to GenBank were T, A, T, T, C, and T, which were the same as those of Pt5 and Pt10, indicating that Pt11 belongs to genotype C (De Martino et al. 2007; Rastogi et al. 2019). The phylogenetic tree based on ITS2 sequences of 11 *P. tricornutum* strains was generated by the neighbor-joining method with 1000 bootstrap replicates (Fig. 1c). Based on this ITS2 phylogenetic tree, Pt1, Pt4, Pt8, and Pt11 represent four different *P. tricornutum* genotypes.

Carbonate system

The carbonate systems in ambient CO_2 (AC, 410 μatm) and high CO_2 (HC, 1000 μatm) cultures were stable with a fluctuation range less than 4.6% by aerating with ambient air and premixed air-CO_2, respectively (Supporting Information Table S2). The carbonate system of HC cultures had 7% higher DIC, 11% higher HCO_3^-, 150% higher CO_2, and 49% lower CO_3^{2-} than the AC treatments (Supporting Information Table S2).

Morphology, growth rate, and pigment contents

Cells cultured in the HC treatments did not differ in their morphology, growth rates, or pigment contents compared to AC cultured cells, in any strains. However, significant differences were observed among different strains ($p < 0.05$). The cells were fusiform under both the AC and HC conditions, with varied length, width, and cell volume among four strains (Supporting Information Table S3). The specific growth rate was the highest in Pt11, and lowest in Pt4 and Pt8 (Supporting Information Fig. S1). Variation in pigment contents between these strains was detected on both per-cell and per-cell-volume basis ($p < 0.05$; Supporting Information Fig. S2). The order of cellular Chl *a* contents on per-cell basis from high to low was similar with that of cellular carotenoid contents, which was Pt11, Pt4, Pt8, and Pt1, both in the AC and HC conditions. Both Chl *a* and carotenoid contents on per-cell-volume basis were the lowest in Pt1, and no significant differences were observed in the other three strains.

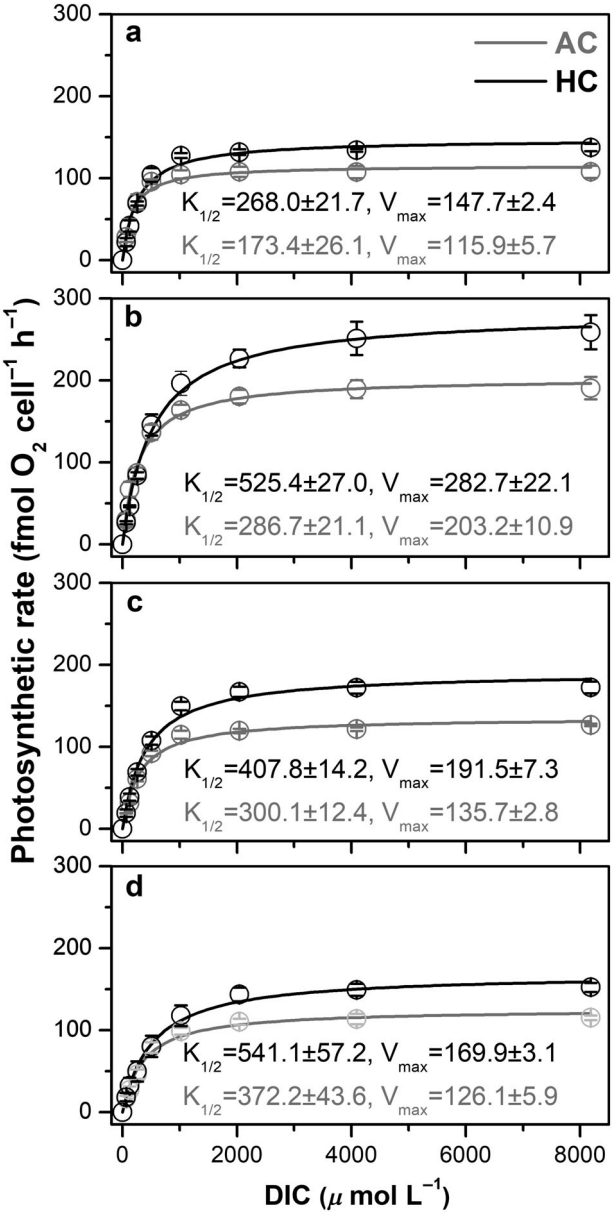

Fig. 2. Photosynthetic oxygen evolution rate response curves of AC- and HC-acclimated cells as a function of DIC concentration for four *P. tricornutum* strains (**a**: Pt1, **b**: Pt4, **c**: Pt8, and **d**: Pt11). Text on each panel described half-saturation constants ($K_{1/2}$, μmol L^{-1} DIC) and maximum DIC-saturated photosynthetic oxygen evolution rates (V_{max}, fmol O_2 $cell^{-1}$ h^{-1}) of AC and HC acclimated cells.

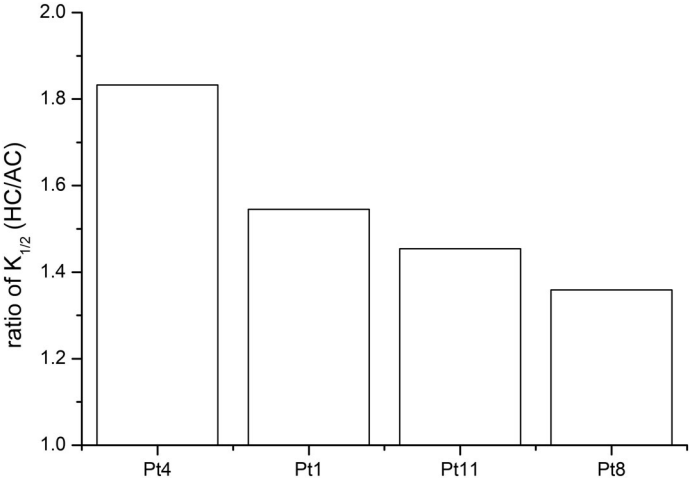

Fig. 3. The ratio of the half saturation constants ($K_{1/2}$ [DIC] for photosynthetic oxygen evolution) in HC-grown cells compared to those in AC-grown cells of four *P. tricornutum* strains.

Kinetics of carbon utilization

The kinetic constants $K_{1/2}$ and V_{max} derived from P-C curves of the four strains tested are shown in Fig. 2, indicating the responses of net photosynthetic oxygen evolution to increased DIC in the AC and HC grown cells. Under AC conditions, $K_{1/2}$ values of these four strains varied within an approximately 2.2-fold range. The variation in V_{max} of these four strains was less than that of $K_{1/2}$ but still substantial, ranging from 115.9 ± 5.7 fmol O_2 $cell^{-1}$ h^{-1} (Pt1) to 203.2 ± 10.9 fmol O_2 $cell^{-1}$ h^{-1} (Pt4) ($p < 0.05$). Although V_{max} and $K_{1/2}$ were increased under the HC conditions, the magnitudes of increase in V_{max} and $K_{1/2}$ were different among these strains. Compared to AC grown cells, the V_{max} of HC cultured cells increased by 27.5–44.2% ($p < 0.05$). The $K_{1/2}$ of HC cultured cells increased by 83.2% in Pt4 and 35.9–54.5% in other strains compared to AC conditions ($p < 0.05$; Fig. 3).

Transcriptional variations in some genes involved in carbon utilization

To explore the changes in HCO_3^- uptake from the environment and CO_2 supply for carbon fixation in response to ocean acidification, we tested the expressional changes of genes encoding plasma membrane HCO_3^- transporters and CAs around Rubisco in AC and HC cultured cells. In addition, the expressional changes of genes encoding C4-like metabolism enzymes were measured, to study the variations of C4-like metabolism in different strains. Variations in the expression changes of these genes in response to HC in different strains are shown in Fig. 4 and Supporting Information Table S4. Compared to AC grown cells, the downregulated expression of bicarbonate transporters PtSLC4-5 (Phatr3_J54405) and PtSLC4-2 (Phatr3_Jdraft1806) in the HC grown cells was only detected in Pt4, with 34% and 96% decrease, respectively. Varied transcriptional patterns of genes encoding critical CAs, PtCA1 (Phatr3_J51305), and PtCA2 (Phatr3_J45443) belonging to β-CAs and Pt43233 (Phatr3_J43233) belonging to θ-CA, in response to high CO_2 were observed in different strains. Under the HC conditions, the expression of PtCA1 was downregulated by 34%, 30%, and 40% in Pt1, Pt8, and Pt11, respectively; PtCA2 was downregulated by 23% in Pt1 and 75% in Pt4; Pt43233 was downregulated by 44% in Pt1 but upregulated by 61% in Pt11. However, HC did not

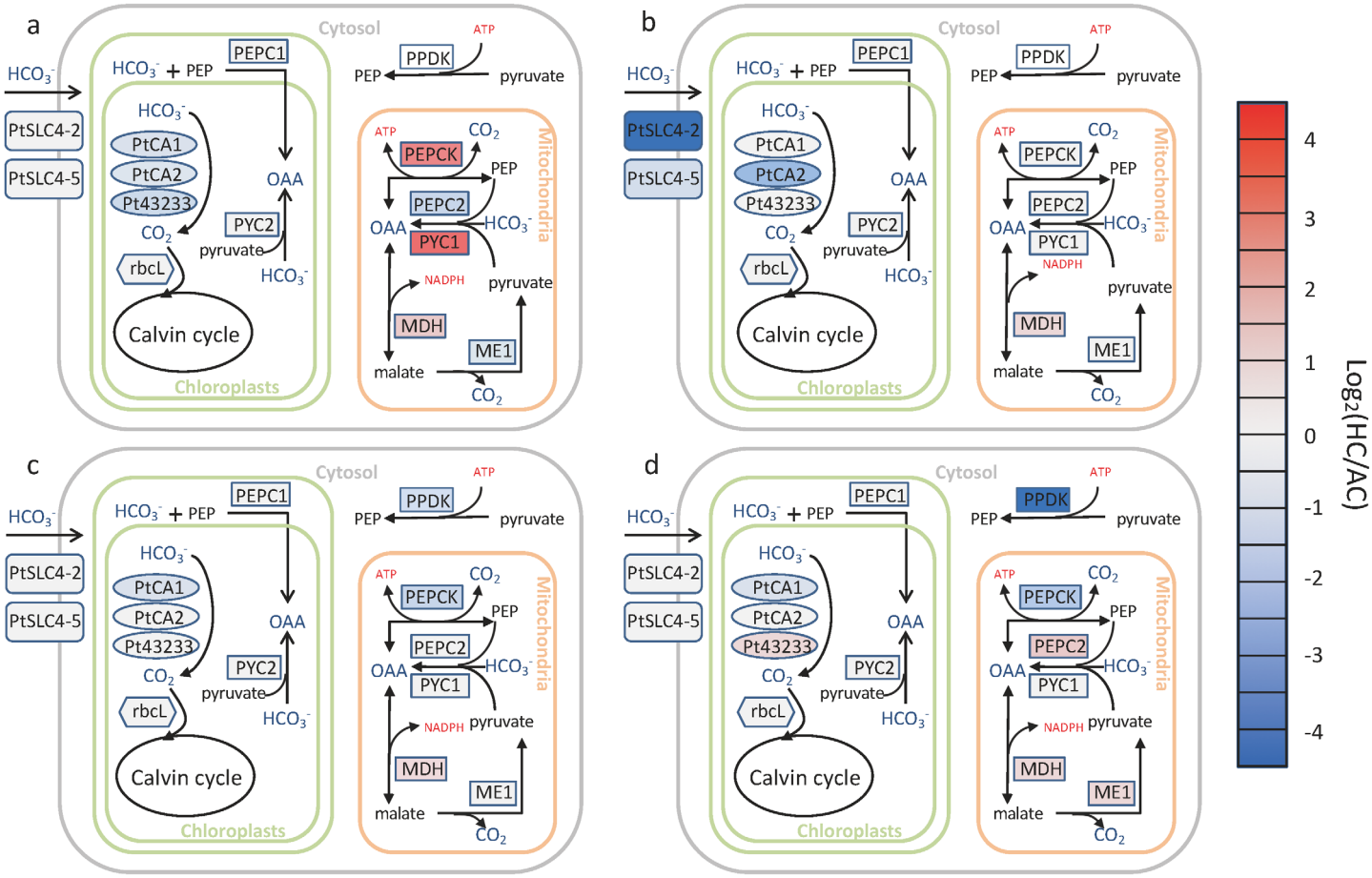

Fig. 4. Expression pattern of genes involved in biophysical CCMs and C4-like metabolism in four *P. tricornutum* strains (**a**: Pt1, **b**: Pt4, **c**: Pt8, and **d**: Pt11) after acclimation for 15 generations. Gene expression changes in high CO_2 experiments relative to ambient CO_2 indicated by heat map (log2 foldchange). SLC4, solute carrier 4 bicarbonate transporters; rbcL, ribulose-1,5-biphosphate carboxylase/oxygenase (Rubisco) large subunit; ME1, NAD^+-malic enzyme.

significantly downregulate the expression of Rubisco large subunit (rbcL) in any strains ($p > 0.05$). In addition, some genes involved in C4-like metabolism showed varied expression patterns in response to the HC conditions in different strains: pyruvate carboxylase 1 (PYC1) was upregulated in Pt1; phosphoenolpyruvate carboxylase 2 (PEPC2) was downregulated in Pt1 but upregulated in Pt11; phosphoenolpyruvate carboxykinase (PEPCK) was upregulated in Pt1 but downregulated in Pt8 and Pt11; PPDK was downregulated in Pt8 and Pt11; malate dehydrogenase (MDH) was upregulated in all strains; NAD^+-malic enzyme (ME1) was downregulated in Pt1 but upregulated in Pt11.

Discussion

Previous studies have shown that the effects of ocean acidification on diatoms are not only regulated by other environmental factors, but also determined by species-specific physiological characteristics (Gao and Campbell 2014). Here, we show that ocean acidification did not significantly influence pigment contents or specific growth rates, probably resulting from balance of energy consumption and production in carbon metabolism (Wu et al. 2010; Gao et al. 2012), in spite of the changes at the transcriptional level (Huang et al. 2018). Both photosynthesis and dark respiration were enhanced under HC conditions, leading to an approximately 5% increase in daily net production (Wu et al. 2010). Energy saved by reduction in carbon acquisition under the HC conditions may be expended by nonphotochemical quenching and photorespiration to protect diatoms from damage (Gao et al. 2012).

Previous studies have shown that changes in seawater CO_2 and HCO_3^- under the HC conditions furthermore influence CCMs at both physiological and molecular levels (Hopkinson et al. 2016; Tsuji et al. 2017). In this study, the expression of tested genes encoding proteins that take part in HCO_3^- uptake and interconversion of CO_2 and HCO_3^- were found to display different patterns, which may result in variable decreased

magnitudes of CO_2 and/or HCO_3^- affinity among different strains. Meanwhile, the elevated CO_2 did not influence the expression of genes encoding the C4-like metabolism enzymes PEPC1 or PYC2 localized in the chloroplasts, but altered C4-like metabolism enzymes localized in mitochondria and cytoplasm. These results suggest that C4-like metabolism may redistribute carbon flux in the mitochondria in response to the HC treatment, rather than participate in carbon fixation. Neither the decrease in CO_2 and/or HCO_3^- affinity, nor the expression pattern of genes involved in CCMs and C4-like metabolism were phylogenetically related, implying that distinct strategies in response to ocean acidification may also be driven by constitutive adaptation to the different environments where the strains were derived (Bailleul et al. 2010).

To overcome limited CO_2 availability for carboxylation, diatoms have evolved CCMs that are distinct from other algae (Matsuda and Kroth 2014) even among different diatom species (Hopkinson et al. 2016; Tsuji et al. 2017). In this study, the affinity for CO_2 and/or HCO_3^- decreased due to altered carbonate chemistry under the HC conditions was observed in all four strains. The magnitudes of DIC affinity reduction were varied among these four strains, implying that strains of the same species may develop different strategies to respond to ocean acidification. *Phaeodactylum tricornutum* can take up both HCO_3^- and CO_2 from the environment, and CO_2 uptake exceeds HCO_3^- uptake by a factor of 2 (Burkhardt et al. 2001). To date, PtSLC4-2, localized in the plasma membrane, has been confirmed as a HCO_3^- transporter, and five putative plasma membrane-type HCO_3^- transporters belonging to SLC4 family have been identified in the genome of *P. tricornutum*. The expression of PtSLC4-5 was down-regulated under 5% CO_2 (50,000 ppmv) conditions and upregulated by 22-fold when exogenous DIC was low (Valenzuela et al. 2012; Nakajima et al. 2013; Matsuda et al. 2017). In the current study, the expression of PtSLC4-2 and PtSLC4-5 was down-regulated in Pt4 in response to elevated CO_2 compared to the ambient CO_2 concentration, but not significantly affected in the other three strains. Our results suggest that repression of HCO_3^- transport in strain Pt4 may be a distinct carbon acquisition strategy in response to ocean acidification, resulting in the largest decrease in DIC affinity compared to other strains (Figs. 3, 4).

Active transport of DIC into the chloroplasts constitutes the main driver of CCMs. Pyrenoids with low permeability to CO_2 play critical roles in concentrating CO_2, where confinement of CA with Rubisco increases the efficiency of the CCMs which can be indicated by $1/K_{1/2}$ (Hopkinson et al. 2011). Among all CAs, the expression of genes encoding β–CAs (PtCA1 and PtCA2) localized in the pyrenoids, as well as one θ-CA (Pt43233) targeted to pyrenoid-penetrating thylakoid lumen, was downregulated by 5% CO_2 which is 50 times higher than 1000 μatm CO_2 used in our experiments (Tachibana et al. 2011; Kikutani et al. 2016). The general decreased expression of genes encoding CAs localized in pyrenoids and pyrenoid-penetrating thylakoid lumen may play a major role in downregulating CCMs in all four strains under the HC conditions (Fig. 5).

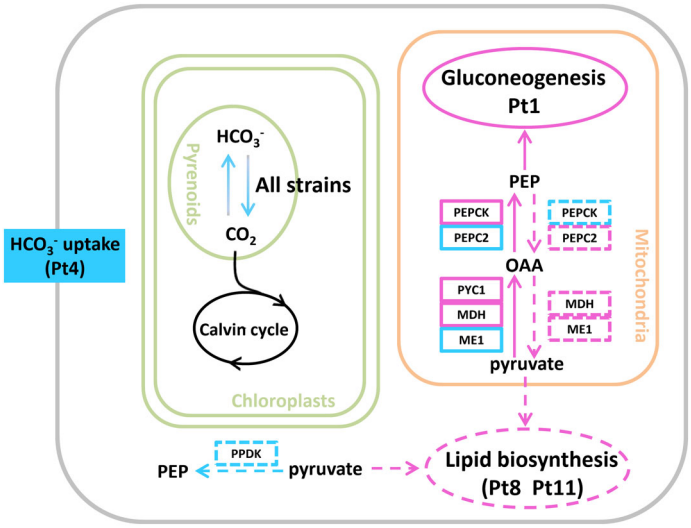

Fig. 5. The schematic model of CCMs and carbon flux changes in C4-like metabolism of four *P. tricornutum* strains under the HC with respect to the AC based on gene expression. Blue and pink colors indicate downregulation and upregulation, respectively. Solid lines in C4-like metabolisms indicate carbon flux in Pt1, and dash lines indicate that of Pt8 and Pt11.

It has been reported that CO_2/cAMP-responsive elements (CCREs) in the promoters of PtCA1 and PtCA2 are critical for responding to CO_2 alterations by a cAMP-mediated signal pathway (Ohno et al. 2012; Tanaka et al. 2016). We also identified that CCRE1 and CCRE2 are in the upstream regulatory region of Pt43233 in Pt1. The decreased expression of genes encoding these CAs in Pt1 may therefore be attributed to the responses of CCREs in the upstream regulatory regions of CA genes. CCRE motifs are highly conserved in Pt43233, PtCA1 and PtCA2 among different strains. The variation in the changes of expression of CAs among other strains may result from different degrees of sensitivity of CAs to CO_2, probably due to nucleotide polymorphism of promoter regions of CAs in different strains.

The C4-type pathway that indirectly participates in carbon fixation is defined as a biochemical CCM. This has been controversial and considered to be limited to particular diatoms (Roberts et al. 2007; Hopkinson et al. 2016). PEPC1 and PYC2, localized in the chloroplasts, are thought to be involved in catalyzing carboxylation of HCO_3^- to oxaloacetic acid (OAA) (Kroth et al. 2008; Ewe et al. 2018). In our study, the genes encoding PEPC1 and PYC2 did not show significant differential expression under the HC conditions in any strains. In addition, to our knowledge, there are no enzymes catalyzing decarboxylation of C4 compounds to CO_2 in the chloroplasts. These results suggest that C4-like metabolism in the chloroplasts may not influence CO_2 fixation. On the other hand, the

expression patterns of genes encoding C4-like metabolism enzymes localized in mitochondria and cytoplasm in Pt8 and Pt11 were similar but distinct from Pt1 and Pt4, which were again not consistent with their phylogenetic relationships (Figs. 4, 5). In Pt4, only the expression of the gene encoding MDH was upregulated. In Pt11, downregulation of PEPCK and upregulation of PEPC2, as well as upregulation of MDH and ME1, may result in carbon flux from phosphoenolpyruvate (PEP) to pyruvate via OAA. Meanwhile, the downregulation of PPDK may suppress the conversion of pyruvate to PEP in the cytoplasm. Possible accumulated pyruvate from PEP and suppression of pyruvate to PEP may further lead to lipid biosynthesis (Yang et al. 2016). The changes in expression of these genes in Pt8 were similar to those observed in Pt11, except that the expression of PEPC2 and ME1 was not significantly affected by the HC treatment. However, in Pt1, the expression of genes encoding enzymes PEPCK, PEPC2, and ME1 was regulated in the opposite direction compared to that in Pt11. The expression of MDH and PYC1 was upregulated, which may also facilitate carbon flux from pyruvate to PEP via OAA. The carbon flux to PEP may further drive gluconeogenesis, since all the enzymes needed for the initial steps of gluconeogenesis can be found in the mitochondria (Ewe et al. 2018). Our results suggest that C4-like metabolism may redistribute carbon flux from carboxylation of HCO_3^- and pyruvate/PEP in response to ocean acidification in different ways in the different strains. Our results also suggest that C4-like metabolism may not participate in net CO_2 fixation, because it is highly unlikely that CO_2, produced via decarboxylation of OAA by PEPCK in Pt1 or decarboxylation of malate by ME1 in Pt11, can permeate from the mitochondria to the chloroplasts through a total of six membranes (Ewe et al. 2018).

It has been supposed that environmental demands drive the evolution of distinct DIC uptake strategies in diatoms (Tsuji et al. 2017). In Antarctic diatoms, HCO_3^- uptake contributes 59–100% of net carbon fixation, and high extracellular CA activity is of particular importance for converting CO_2 to HCO_3^- that is subsequently taken up by HCO_3^- transporters (Trimborn et al. 2013). The CO_2 concentration in seawater is determined by pCO_2 and solubility of CO_2 in Henry's law, in which CO_2 solubility is not only negatively influenced by temperature but also dependent on salinity (Zeebe and Wolf-Gladrow 2001; Young et al. 2015). According to the Copernicus-Marine environment monitoring service (CMEMS) database, the average CO_2 concentration of the seawater in which Pt4 was isolated is approximately 15 μmol L^{-1}, which is nearly equal to the environment where Pt1 was isolated, and lower than that of Pt8 (Supporting Information Table S5). Because of the lower CO_2 diffusion at lower temperatures (a factor of 2 between 20°C and 0°C; Kranz et al. 2015), and lack of extracellular interconversion between CO_2 and HCO_3^- by extracellular CAs (Tachibana et al. 2011; Kikutani et al. 2016), the HCO_3^- : CO_2 uptake ratio of the coldest adapted Pt4 may be greater than that of other strains. It has been reported that the HCO_3^- uptake of polar diatoms inversely correlated with CO_2 concentration (Neven et al. 2011; Kranz et al. 2015). As pCO_2 increases, Pt4 may reduce HCO_3^- acquisition more preferentially than other strains, which would save more energy consumed by CCMs. However, the strains used in this study have been transferred from their local natural environment to laboratory conditions for several decades, in which evolutionary processes do not cease to occur (Lakeman et al. 2009; Pargana et al. 2020). Therefore, to better explore strain-specific response to ocean acidification, molecular and physiological experiments in both laboratory and field should be conducted using more recently isolated strains in the future.

Our results demonstrate that increased concentrations of pCO_2 in seawater relevant to ocean acidification influence the model diatom's inorganic carbon acquisition capability and C4-like metabolism, with strain-specific differences as large as those previously observed between species. In addition, the variation in responses among strains was not in line with phylogenetic relationship based on ITS2 sequences, implying that the environment-adapted traits might also play important roles in driving diatoms to adopt strategies to deal with changing ocean chemistry. In the future, more comprehensive analysis, such as integrated analysis of environment-functional genes-physiological performance, using more recently isolated strains from distinct habitats, is needed to better illustrate this point. The current research thus suggests that strain-specific responses should not be neglected in considering effects of ocean climate change on diatoms. Variation in the responses of strains to ocean acidification and other environmental factors will likely influence species niches, ecosystem composition, and element biogeochemical cycles in different ocean regions.

References

Abida, H., and others. 2015. Membrane glycerolipid remodeling triggered by nitrogen and phosphorus starvation in *Phaeodactylum tricornutum*. Plant Physiol. **167**: 118–136. doi:10.1104/pp.114.252395

Badger, M. R., and others. 1998. The diversity and coevolution of Rubisco, plastids, pyrenoids, and chloroplast-based CO_2-concentrating mechanisms in algae. Can. J. Bot. **76**: 1052–1071. doi:10.1139/b98-074

Bailleul, B., and others. 2010. An atypical member of the light-harvesting complex stress-related protein family modulates diatom responses to light. Proc. Natl. Acad. Sci. USA **107**: 18214–18219. doi:10.1073/pnas.1007703107

Burkhardt, S., G. Amoroso, U. Riebesell, and D. Sültemeyer. 2001. CO_2 and HCO_3^- uptake in marine diatoms acclimated to different CO_2 concentrations. Limnol. Oceanogr. **46**: 1378–1391. doi:10.4319/lo.2001.46.6.1378

De Martino, A., A. Meichenin, J. Shi, K. Pan, and C. Bowler. 2007. Genetic and phenotypic characterization of

Phaeodactylum tricornutum (Bacillariophyceae) accessions. J. Phycol. **43**: 992–1009. doi:10.1111/j.1529-8817.2007.00384.x

De Martino, A., and others. 2011. Physiological and molecular evidence that environmental changes elicit morphological interconversion in the model diatom *Phaeodactylum tricornutum*. Protist **162**: 462–481. doi:10.1016/j.protis.2011.02.002

Ewe, D., and others. 2018. The intracellular distribution of inorganic carbon fixing enzymes does not support the presence of a C4 pathway in the diatom *Phaeodactylum tricornutum*. Photosynth. Res. **137**: 263–280. doi:10.1007/s11120-018-0500-5

Gao, K., and others. 2012. Rising CO_2 and increased light exposure synergistically reduce marine primary productivity. Nat. Clim. Chang. **2**: 519–523. doi:10.1038/nclimate1507

Gao, K., and D. A. Campbell. 2014. Photophysiological responses of marine diatoms to elevated CO_2 and decreased pH: A review. Funct. Plant Biol. **41**: 449–459. doi:10.1071/fp13247

Gattuso, J.-P., and others. 2015. Contrasting futures for ocean and society from different anthropogenic CO_2 emissions scenarios. Science **349**: aac4722. doi:10.1126/science.aac4722

Gehlen, M., N. Gruber, R. Gangstø, L. Bopp, and A. Oschlies. 2011. Biogeochemical consequences of ocean acidification and feedbacks to the earth system, p. 230–248. *In* J.-P. Gattuso and L. Hansson [eds.], Ocean acidification. Oxford Univ. Press.

Haimovich-Dayan, M., and others. 2013. The role of C4 metabolism in the marine diatom *Phaeodactylum tricornutum*. New Phytol. **197**: 177–185. doi:10.1111/j.1469-8137.2012.04375.x

Hillebrand, H., C.-D. Dürselen, D. Kirschtel, U. Pollingher, and T. Zohary. 1999. Biovolume calculation for pelagic and benthic microalgae. J. Phycol. **35**: 403–424. doi:10.1046/j.1529-8817.1999.3520403.x

Hopkinson, B. M., C. L. Dupont, A. E. Allen, and F. M. M. Morel. 2011. Efficiency of the CO_2-concentrating mechanism of diatoms. Proc. Natl. Acad. Sci. USA **108**: 3830–3837. doi:10.1073/pnas.1018062108

Hopkinson, B. M., C. L. Dupont, and Y. Matsuda. 2016. The physiology and genetics of CO_2 concentrating mechanisms in model diatoms. Curr. Opin. Plant Biol. **31**: 51–57. doi:10.1016/j.pbi.2016.03.013

Hoppe, C. J., L. M. Holtz, S. Trimborn, and B. Rost. 2015. Ocean acidification decreases the light-use efficiency in an Antarctic diatom under dynamic but not constant light. New Phytol. **207**: 159–171. doi:10.1111/nph.13334

Huang, R., and others. 2019. A potential role for epigenetic processes in the acclimation response to elevated pCO_2 in the model diatom *Phaeodactylum tricornutum*. Front. Microbiol. **9**: 3342. doi:10.3389/fmicb.2018.03342

Hutchins, D. A., F.-X. Fu, E. A. Webb, N. Walworth, and A. Tagliabue. 2013. Taxon-specific response of marine nitrogen fixers to elevated carbon dioxide concentrations. Nat. Geosci. **6**: 790–795. doi:10.1038/ngeo1858

Kiene, R. P. 2008. Marine biology: Genes in the glass house. Nature **456**: 179–181. doi:10.1038/456179a

Kikutani, S., K. Nakajima, C. Nagasato, Y. Tsuji, A. Miyatake, and Y. Matsuda. 2016. Thylakoid luminal θ-carbonic anhydrase critical for growth and photosynthesis in the marine diatom *Phaeodactylum tricornutum*. Proc. Natl. Acad. Sci. USA **113**: 9828–9833. doi:10.1073/pnas.1603112113

Kranz, S. A., J. N. Young, B. M. Hopkinson, J. A. Goldman, P. D. Tortell, and F. M. Morel. 2015. Low temperature reduces the energetic requirement for the CO_2 concentrating mechanism in diatoms. New Phytol. **205**: 192–201. doi:10.1111/nph.12976

Kroeker, K. J., and others. 2013. Impacts of ocean acidification on marine organisms: Quantifying sensitivities and interaction with warming. Glob. Chang. Biol. **19**: 1884–1896. doi:10.1111/gcb.12179

Kroth, P. G., and others. 2008. A model for carbohydrate metabolism in the diatom *Phaeodactylum tricornutum* deduced from comparative whole genome analysis. PLoS One **3**: e1426. doi:10.1371/journal.pone.0001426

Kustka, A. B., and others. 2014. Low CO_2 results in a rearrangement of carbon metabolism to support C4 photosynthetic carbon assimilation in *Thalassiosira pseudonana*. New Phytol. **204**: 507–520. doi:10.1111/nph.12926

Lakeman, M. B., P. von Dassow, and R. A. Cattolico. 2009. The strain concept in phytoplankton ecology. Harmful Algae **8**: 746–758. doi:10.1016/j.hal.2008.11.011

Langer, G., G. Nehrke, I. Probert, J. Ly, and P. Ziveri. 2009. Strain-specific responses of *Emiliania huxleyi* to changing seawater carbonate chemistry. Biogeosciences **6**: 2637–2646. doi:10.5194/bg-6-2637-2009

Li, F., Y. Wu, D. A. Hutchins, F. Fu, and K. Gao. 2016. Physiological responses of coastal and oceanic diatoms to diurnal fluctuations in seawater carbonate chemistry under two CO_2 concentrations. Biogeosciences **13**: 6247–6259. doi:10.5194/bg-13-6247-2016

Li, F., J. Beardall, and K. Gao. 2018. Diatom performance in a future ocean: Interactions between nitrogen limitation, temperature, and CO_2-induced seawater acidification. ICES J. Mar. Sci. **75**: 1451–1464. doi:10.1093/icesjms/fsx239

Li, W., K. Gao, and J. Beardall. 2015. Nitrate limitation and ocean acidification interact with UV-B to reduce photosynthetic performance in the diatom *Phaeodactylum tricornutum*. Biogeosciences **12**: 2383–2393. doi:10.5194/bg-12-2383-2015

Li, Y., K. Gao, V. E. Villafañe, and E. W. Helbling. 2012. Ocean acidification mediates photosynthetic response to UV radiation and temperature increase in the diatom *Phaeodactylum tricornutum*. Biogeosciences **9**: 3931–3942. doi:10.5194/bg-9-3931-2012

Li, Y., J. Xu, and K. Gao. 2014. Light-modulated responses of growth and photosynthetic performance to ocean acidification in the model diatom *Phaeodactylum tricornutum*. PLoS One **9**: e96173. doi:10.1371/journal.pone.0096173

Liu, N., J. Beardall, and K. Gao. 2017. Elevated CO_2 and associated seawater chemistry do not benefit a model diatom grown with increased availability of light. Aquat. Microb. Ecol. **79**: 137–147. doi:10.3354/ame01820

Matsuda, Y., and P. G. Kroth. 2014. Carbon fixation in diatoms, p. 335–362. *In* M. F. Hohmann-Marriott [ed.], The structural basis of biological energy generation. Springer.

Matsuda, Y., B. M. Hopkinson, K. Nakajima, C. L. Dupont, and Y. Tsuji. 2017. Mechanisms of carbon dioxide acquisition and CO_2 sensing in marine diatoms: A gateway to carbon metabolism. Philos. Trans. R. Soc. Lond. B Biol. Sci. **372**: 20160403. doi:10.1098/rstb.2016.0403

McCarthy, A., S. P. Rogers, S. J. Duffy, and D. A. Campbell. 2012. Elevated carbon dioxide differentially alters the photophysiology of *Thalassiosira pseudonana* (Bacillariophyceae) and *Emiliania Huxleyi* (Haptophyta). J. Phycol. **48**: 635–646. doi:10.1111/j.1529-8817.2012.01171.x

Müller, M. N., T. W. Trull, and G. M. Hallegraeff. 2015. Differing responses of three Southern Ocean *Emiliania huxleyi* ecotypes to changing seawater carbonate chemistry. Mar. Ecol. Prog. Ser. **531**: 81–90. doi:10.3354/meps11309

Nakajima, K., A. Tanaka, and Y. Matsuda. 2013. SLC4 family transporters in a marine diatom directly pump bicarbonate from seawater. Proc. Natl. Acad. Sci. USA **110**: 1767–1772. doi:10.1073/pnas.1216234110

Neven, I. A., J. Stefels, S. M. A. C. van Heuven, H. J. W. de Baar, and J. T. M. Elzenga. 2011. High plasticity in inorganic carbon uptake by Southern Ocean phytoplankton in response to ambient CO_2. Deep-Sea Res. Part II Top. Stud. Oceanogr. **58**: 2636–2646. doi:10.1016/j.dsr2.2011.03.006

Ohno, N., and others. 2012. CO_2-cAMP-responsive cis-elements targeted by a transcription factor with CREB/ATF-like basic zipper domain in the marine diatom *Phaeodactylum tricornutum*. Plant Physiol. **158**: 499–513. doi:10.1104/pp.111.190249

Pargana, A., and others. 2020. Intraspecific diversity in the cold stress response of transposable elements in the diatom *Leptocylindrus aporus*. Genes **11**: 9. doi:10.3390/genes11010009

Rastogi, A., and others. 2019. A genomics approach reveals the global genetic polymorphism, structure, and functional diversity of ten accessions of the marine model diatom *Phaeodactylum tricornutum*. ISME J. **14**: 347–363. doi:10.1038/s41396-019-0528-3

Raven, J. A., and J. Beardall. 2016. The ins and outs of CO_2. J. Exp. Bot. **67**: 1–13. doi:10.1093/jxb/erv451

Reinfelder, J. R., A. M. L. Kraepiel, and F. M. M. Morel. 2000. Unicellular C4 photosynthesis in a marine diatom. Nature **407**: 996–999. doi:10.1038/35039612

Ritchie, R. J. 2006. Consistent sets of spectrophotometric chlorophyll equations for acetone, methanol and ethanol solvents. Photosynth. Res. **89**: 27–41. doi:10.1007/s11120-006-9065-9

Roberts, K., E. Granum, R. C. Leegood, and J. A. Raven. 2007. C3 and C4 pathways of photosynthetic carbon assimilation in marine diatoms are under genetic, not environmental, control. Plant Physiol. **145**: 230–235. doi:10.1104/pp.107.102616

Schaum, E., B. Rost, A. J. Millar, and S. Collins. 2012. Variation in plastic responses of a globally distributed picoplankton species to ocean acidification. Nat. Clim. Chang. **3**: 298–302. doi:10.1038/nclimate1774

Siaut, M., and others. 2007. Molecular toolbox for studying diatom biology in *Phaeodactylum tricornutum*. Gene **406**: 23–35. doi:10.1016/j.gene.2007.05.022

Strickland, J. D. H., and T. R. Parsons. 1972. A practical handbook of seawater analysis. Fisheries Research Board of Canada.

Tachibana, M., A. E. Allen, S. Kikutani, Y. Endo, C. Bowler, and Y. Matsuda. 2011. Localization of putative carbonic anhydrases in two marine diatoms, *Phaeodactylum tricornutum* and *Thalassiosira pseudonana*. Photosynth. Res. **109**: 205–221. doi:10.1007/s11120-011-9634-4

Tanaka, A., N. Ohno, K. Nakajima, and Y. Matsuda. 2016. Light and CO_2/cAMP signal cross talk on the promoter elements of chloroplastic b-carbonic anhydrase genes in the marine diatom *Phaeodactylum tricornutum*. Plant Physiol. **170**: 1105–1116. doi:10.1104/pp.15.01738

Torstensson, A., M. Hedblom, J. Andersson, M. X. Andersson, and A. Wulff. 2013. Synergism between elevated pCO_2 and temperature on the Antarctic Sea ice diatom *Nitzschia lecointei*. Biogeosciences **10**: 6391–6401. doi:10.5194/bg-10-6391-2013

Trimborn, S., T. Brenneis, E. Sweet, and B. Rost. 2013. Sensitivity of Antarctic phytoplankton species to ocean acidification: Growth, carbon acquisition, and species interaction. Limnol. Oceanogr. **58**: 997–1007. doi:10.4319/lo.2013.58.3.0997

Tsuji, Y., A. Mahardika, and Y. Matsuda. 2017. Evolutionarily distinct strategies for the acquisition of inorganic carbon from seawater in marine diatoms. J. Exp. Bot. **68**: 3949–3958. doi:10.1093/jxb/erx102

Valenzuela, J., A. Mazurie, R. P. Carlson, R. Gerlach, K. E. Cooksey, B. M. Peyton, and M. W. Fields. 2012. Potential role of multiple carbon fixation pathways during lipid accumulation in *Phaeodactylum tricornutum*. Biotechnol. Biofuels **5**: 40. doi:10.1186/1754-6834-5-40

Wu, Y., K. Gao, and U. Riebesell. 2010. CO_2-induced seawater acidification affects physiological performance of the marine diatom *Phaeodactylum tricornutum*. Biogeosciences **7**: 2915–2923. doi:10.4319/lo.2014.59.3.1027

Yang, J., Y. Pan, C. Bowler, L. Zhang, and H. Hu. 2016. Knockdown of phosphoenolpyruvate carboxykinase increases

carbon flux to lipid synthesis in *Phaeodactylum tricornutum*. Algal Res. **15**: 50–58. doi:10.1016/j.algal.2016.02.004

Young, J. N., S. A. Kranz, J. A. L. Goldman, P. D. Tortell, and F. M. M. Morel. 2015. Antarctic phytoplankton down-regulate their carbon-concentrating mechanisms under high CO_2 with no change in growth rates. Mar. Ecol. Prog. Ser. **532**: 13–28. doi:10.3354/meps11336

Young, J. N., A. M. Heureux, R. E. Sharwood, R. E. Rickaby, F. M. Morel, and S. M. Whitney. 2016. Large variation in the Rubisco kinetics of diatoms reveals diversity among their carbon-concentrating mechanisms. J. Exp. Bot. **67**: 3445–3456. doi:10.1093/jxb/erw163

Zeebe, R. E., and D. Wolf-Gladrow. 2001. CO_2 in seawater: Equilibrium, kinetics, isotopes. Elsevier.

Zhang, Y., and others. 2014. Between- and within-population variations in thermal reaction norms of the coccolithophore *Emiliania huxleyi*. Limnol. Oceanogr. **59**: 1570–1580. doi:10.4319/lo.2014.59.5.1570

Acknowledgments

This study was supported by National Natural Science Foundation of China (41720104005 and 41721005 to K.G. and 41306096 to X.L.), Joint project of National Natural Science Foundation of China and Shandong province (U1606404), and National Key Research and Development Program of China (2016YFA0601302). We thank Jason Hall-Spencer for his relevant advice and Jonathan Adams for correcting the grammatical mistakes. We also thank Wenyan Zhao and Xianglan Zeng for their kind assistance in this research.

Conflict of Interest

None declared.

Submitted 03 May 2019
Revised 28 November 2019
Accepted 09 June 2020

Associate editor: Tatiana Rynearson